



# The influence of temperature on autogenous volume changes in cementitious materials containing shrinkage reducing admixtures

Gaurav Sant\*

Laboratory for the Chemistry of Construction Materials, Department of Civil and Environmental Engineering, 420 Westwood Plaza, 5731-J Boelter Hall, University of California, Los Angeles, CA 90095, USA

## ARTICLE INFO

### Article history:

Received 20 May 2011

Received in revised form 3 April 2012

Accepted 6 April 2012

Available online 18 April 2012

### Keywords:

Cracking

Relative humidity (RH)

Residual stress

Autogenous shrinkage

Temperature

Shrinkage reducing admixture (SRA)

Maturity transformations

## ABSTRACT

This research examines the influence of temperature on unrestrained and restrained autogenous volume changes in cementitious systems containing shrinkage reducing admixtures (SRAs). The apparent activation energy of cement hydration is determined using measurements of isothermal conduction calorimetry. Time-temperature (equivalent-age based) transformations are applied to extract the apparent activation energy of cement hydration (reactions). The results indicate that while equivalent-age transformations are a suitable procedure for describing the influence of temperature on chemical reactions, they are an inappropriate approach to describe the evolution of volume changes in cementitious materials cured at different temperatures. It is noted that while SRAs do not substantially alter the temperature sensitivity of hydration reactions, their ability to induce early-age expansions negates the use of maturity (equivalent age) approaches in describing autogenous deformations in these materials. Efforts are made to better describe the thermodynamic-limitations of autogenous RH change (self-desiccation) and the need to account for viscoelastic (i.e., creep) and damage (i.e., microcracking) considerations in interpreting the residual stress development response of cement-based materials cured at different temperatures.

© 2012 Elsevier Ltd. All rights reserved.

## 1. Introduction and background

The rate of cement hydration increases in proportion with an increase in temperature. This topic has received significant treatment in cement literature [1–4], with the objective of determining a correlation between the temperature, rate and extent of reaction (hydration), and material property development (i.e., strength and elastic modulus [5,6]). Time-temperature transformations (i.e., maturity approaches) have correlated the development of material properties to the extent of hydration [7,8]. Hansen and Pedersen [9] proposed an equivalent-age function (Eq. (1)) to describe the influence of the reaction temperature on property development in cementitious materials cured at various temperatures and determined a value of 33.5 kJ/mol for the activation energy of cement hydration:

$$t_e = \int_0^t \exp \left[ \frac{-E_{aR}}{R} \left( \frac{1}{T} - \frac{1}{T_{REF}} \right) \right] dt \quad (1)$$

where  $t_e$  (hours) is the equivalent age at a reference temperature  $T_{REF}$  (296.15 K in this paper),  $E_{aR}$  (kJ/mol) is the apparent activation energy of the hydration reaction,  $R$  (J/K mol) is the ideal gas constant (8.314 J/K mol),  $T$  (K) is the curing temperature that can vary in time, and  $t$  is the actual specimen age (hours).

The theoretical concept of an activation energy [10] is strictly applicable only for single reaction systems where the kinetic energy needed for the progression of the (singular) forward reaction is a well-defined value. Since portland cement hydration involves multiple reactions that occur simultaneously and interact with each other, the activation energy described in Eq. (1) is the apparent (effective) activation energy of cement hydration. When the maturity concept is applied to cementitious systems, it is often incorrectly assumed that the overall response depends only on the extent of reaction and other processes (e.g., self-desiccation) or the microstructure that is formed are not influenced by temperature or the rate at which the reactions occur. For example, specimens cured at 10, 23, or 36 °C to the same maturity (i.e., degree of hydration) are assumed to have the same microstructure. This is incorrect as previous studies have consistently shown that systems reacting at different temperature (at varying reaction rates) form different reaction products with differing spatial arrangements (and thus the porosity) in the system [11,12].

High-performance concrete mixtures generally have a low water-to-cement ratio (w/c) and experience significant self-desiccation and autogenous shrinkage [13,14]. Self-desiccation and external drying in these mixtures both result in the development of capillary stresses which amplify the risk of shrinkage cracking in these systems. Shrinkage reducing admixtures were developed as a “chemical technology” to reduce shrinkage and cracking in restrained concrete elements [15–20]. Being surfactants, SRAs reduce

\* Tel.: +1 310 206 3084; fax: +1 310 206 2222.

E-mail address: [gsant@ucla.edu](mailto:gsant@ucla.edu)

the surface tension of the pore-fluids which acts to limit self-desiccation and capillary stress development [15,16,47,49]. However, in addition to surface tension effects, SRAs also alter the chemistry of the pore solution which acts to induce early-age expansions in these systems [21,46]. The expansion is significant as it can correspond to a majority of the shrinkage reduction in SRA systems, under sealed conditions [28,35,44,46,49]. While, autogenous/drying effects of cementitious materials have been extensively studied, fewer efforts have described the influence of the curing temperature on deformations and stress development at early-ages, especially in systems containing SRAs [22–28]. For example: while previous studies have indicated an unsystematic temperature dependence of autogenous deformations, other research has indicated that the maturity (i.e., the equivalent age) approach is not applicable or applicable over a limited temperature range to predict autogenous deformations in systems cured at varying temperatures [22,25,26]. It has been further suggested that autogenous deformations and residual stress development would depend on the pore structure, whose properties depend on the curing temperature [26].

This paper discusses an extensive set of experimental observations, to describe the applicability of maturity based approaches in the context of interpreting autogenous deformations and stress development in cementitious materials containing shrinkage reducing admixtures (SRAs). It is demonstrated that the application of maturity transformations is inapplicable when aspects other than the cement hydration rate need to be considered; e.g., expansions, self-desiccation, damage and/or viscoelastic effects. The outcomes of this research are relevant in developing modeling methods which can simulate autogenous deformations and residual stress development and predicting the risk/potential of shrinkage cracking in plain and SRA containing concretes cured at different (environmental) temperatures.

## 2. Materials and mixing procedures

Two different cement paste mixtures were prepared as per the mixture proportions shown in Table 1. An ASTM C150 compliant, Type I ordinary portland cement with a Blaine fineness of 360 m<sup>2</sup>/kg and an estimated Bogue phase composition of 60% C<sub>3</sub>S, 12% C<sub>2</sub>S, 12% C<sub>3</sub>A, 7% C<sub>4</sub>AF and a Na<sub>2</sub>O equivalent of 0.72% was used in this study. A high range water reducing admixture (Glenium 3000NS) was added to the cement paste mixtures. For one mixture, a commercially available shrinkage-reducing admixture (Tetraguard AS20) was added by 5% replacement (by mass) of the initial mixing water. The cement paste mixtures were prepared as described in ASTM C305 [29,30].

## 3. Experimental procedures

### 3.1. Isothermal conduction calorimetry

Isothermal conduction calorimetry was performed on duplicate cement paste mixtures using a TamAir isothermal calorimeter to determine the heat dissipated during the hydration reaction under a constant temperature condition (10 °C, 23 °C and 36 °C) and then

used to determine the apparent activation energy of cement hydration. The thermal power and energy measured were used to assess the kinetics and the extent of hydration of the cement paste assuming an ultimate heat release value of 510 J/g for the cement based on its phase composition [31,32].

### 3.2. Autogenous deformation: the corrugated tube method

Linear autogenous strain of cement pastes was measured using a technique where the fresh paste was placed in corrugated polyethylene molds [33]. The corrugated tubes had a length-to-diameter of approximately 400–30 mm. The corrugated mold transforms volumetric deformations into linear deformations when the paste is in a fluid state, since the mold has a greater stiffness in the radial direction than in the longitudinal direction. The technique is designed to encapsulate the fresh cement paste while minimizing restraint, thereby permitting measurements to start soon after casting (i.e., approximately 30 min after water addition). The cement paste was cast into corrugated tubes and then vibrated. Duplicate specimens were placed in a dilatometer rig which was placed in an environmental chamber maintained at 10, 23 or 36 °C. The dilatometer was equipped with electronic displacement transducers with an accuracy of  $\pm 5 \mu\text{m/m}$  [29] and was PC interfaced to provide automated data-logging capability. Data acquisition was started around 30 min after water addition. Data was recorded at 5 min intervals for the duration of the test corresponding to an age of 7 days at 23 °C. The measurement results were then zeroed at the time of final set [34].

### 3.3. Residual stress development: the dual ring test

Residual stress development in duplicate cement pastes was measured using a newly developed dual ring setup. The apparatus consisted of two rings (an inner ring and an outer ring) made of Invar-36 to minimize the effects of temperature change on the strain results [35–37]. The inner ring had an outer radius of 50.8 mm and an inner radius of 44.5 mm. The outer invar ring had an outer radius of 82.6 mm and an inner radius of 76.2 mm. Each ring was instrumented with four strain gages placed at 90° from one another at the mid-height on the inner and outer circumference of the inner and outer ring respectively. The height of rings was 25.4 mm. The instrumented rings were placed at the center of an acrylic base, which was lined with acetate sheets and form-release agent to minimize bond and restraint between the base, the invar rings, and the cement paste. Fresh cement paste was then cast between the two rings. The setup was maintained in an environmental chamber at 10, 23 and 36 °C  $\pm 0.1$  °C under nitrogen purge to minimize the potential for carbonation. The restrained strain measurements were recorded at 5-min intervals, starting at 30 min after mixing, until an equivalent age of 7 days. Each strain gage had a measuring resolution of  $\pm 0.01 \mu\text{m/m}$  and each instrumented ring had a typical standard deviation of the measurement of  $\pm 0.25 \mu\text{m/m}$  [35,36].

### 3.4. Autogenous internal equilibrium relative humidity of cement pastes

The internal equilibrium relative humidity (RH) of mature (i.e., well-aged) cement pastes was monitored simultaneously (in duplicate) in the measuring chambers of two Rotronic hygroscope stations equipped with WA-14TH and WA-40TH cells [38]. Each station was equipped with a Pt-100 temperature sensor and a DMS-100H relative humidity sensor. The stations were provided with a fluid-based thermo-regulation system that maintained the each cell's temperature within  $\pm 0.1$  °C. To describe autogenous-RH change as a function of temperature in pastes having a non-

**Table 1**  
Mixture proportions of the cement pastes investigated (mass fractions).

Mixture ID	w/c = 0.30	w/c = 0.30SRA
Water	0.3000	0.2850
Cement	1.0000	1.0000
HRWRA	0.0050	0.0050
SRA	–	0.0150

changing (fixed) microstructure, mature pastes ( $\sim 1$  year old; sealed curing) were crushed and a small amount was placed ( $\sim 10$  g) in the measuring cell of the hygroscope. The relative humidity was then measured at 4, 20 and 35 °C. Prior to measurement, the mature pastes were cured under sealed conditions at room temperature; i.e., 23 °C. Before and after the measurements, calibration of the stations was carried out with four saturated salt solutions ( $K_2SO_4$ ,  $KNO_3$ , KCl, NaCl) with a known constant RH in the range of 75–100% (ASTM E104) at 20 °C. The calibration procedure took 24 h and its implementation yields a global measurement accuracy of  $\pm 1\%$  RH [38].

### 3.5. Surface tension of DI-Water-SRA solutions using a du noüy ring tensiometer

The surface tension of solutions of SRA and de-ionized (DI) water were measured using the du Noüy Ring method over a temperature range of 5–35 °C  $\pm 0.5$  °C [39,40]. This method is based on determining the force that is required to detach a wire ring from the surface of a solution. The ring used was made of a platinum-iridium alloy and was cleaned according to ASTM D971 prior to each measurement. The measured surface tension of distilled water (0.0723 N/m) was used as a standard reference in determining the change in surface tension caused by the addition of the SRA [41]. The average of three measurements was used in the representation of each data-point, with a typical coefficient of variation being 0.50%. A more detailed description of the surface tension measurements can be found elsewhere [42,43].

## 4. Experimental results

### 4.1. Isothermal conduction calorimetry – the rate and extent of cement hydration

Fig. 1 describes the cumulative energy released by the cement pastes cured at 10, 23 and 36 °C measured using isothermal calorimetry. Expectedly, for both pastes, the rate of reaction and the rate of energy released increases with increasing temperature. The magnitude of energy released at an equivalent age of 72 h for both mixtures is similar independent of temperature and corresponds to about 53% hydration for both the plain and SRA mixtures, for measurements performed at 23 °C (Fig. 5 [46]). It should be noted, in order to obtain true material behavior, the cement pastes should be precisely conditioned to the measurement temperature at the end of the mixing cycle [35].

### 4.2. Autogenous deformation of cement pastes

Fig. 2a shows the evolution of autogenous deformation measured using the corrugated tubes from the time of final set in plain cement pastes cured at different temperatures [34]. While the rate of shrinkage is significantly altered by the curing temperature, the magnitude of shrinkage experienced at the end of the testing period is similar ( $\sim 900$   $\mu\text{m/m}$ ) for all curing temperatures. The difference in the rate of shrinkage can be attributed to the temperature dependence of both cement hydration and self-desiccation. It should also be noted that between the time of setting and 72 h,

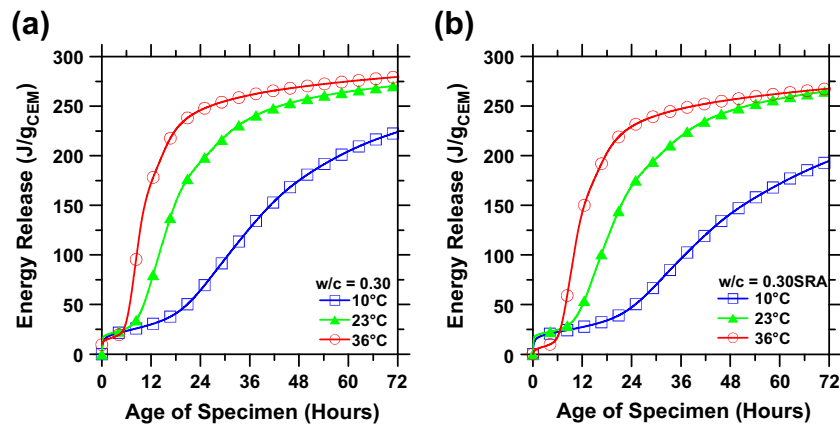


Fig. 1. The cumulative energy release as a function of specimen age for pastes cured at different temperature for: (a) plain pastes and (b) pastes containing SRA.

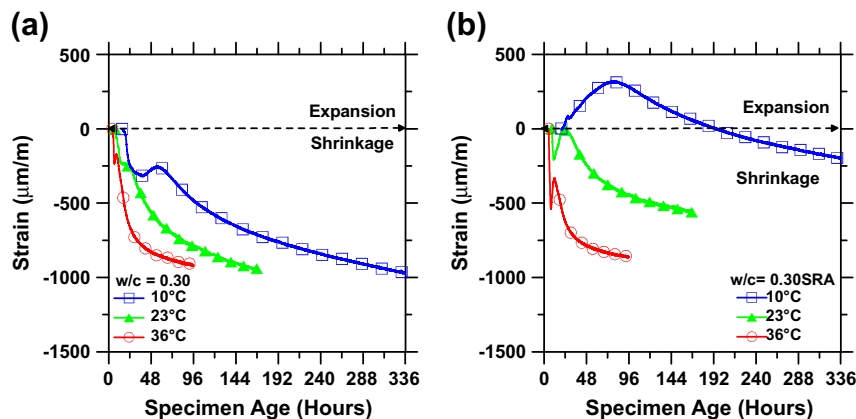


Fig. 2. Autogenous deformation from the time of set as a function of specimen age for cement pastes cured at different temperatures for: (a) plain pastes and (b) SRA containing pastes.

samples cured at 10, 23 and 36 °C show a markedly different behavior. For example: while the sample cured at 23 °C shows a plateau in the development of shrinkage shortly after setting, the samples cured at 10 and 36 °C experience an expansion of approximately 60  $\mu\text{m}/\text{m}$  (although at different time intervals) after the mixture has set.

Fig. 2b shows the evolution of autogenous deformation from the time of final set in pastes containing SRA cured at different temperatures. For these mixtures, the rate and magnitude of deformation shows a large dependence on temperature. In fact, the mixture cured at 10 °C shows a net post-set expansion until approximately 192 h, with a peak expansion of 325  $\mu\text{m}/\text{m}$  while the mixture cured at 23 °C experiences a peak expansion of 235  $\mu\text{m}/\text{m}$  and the mixture cured at 36 °C of 175  $\mu\text{m}/\text{m}$ . The expansion occurring in SRA mixtures has been attributed to the development of crystallization stresses produced by portlandite formation in the system [44–46].

#### 4.3. Residual stress development in cement pastes

Fig. 3a shows the development of residual stresses measured using the dual ring setup in plain mixtures cured at 10, 23, and 36 °C. The mixture cured at 10 °C develops insignificant stresses during the first 24 h after which time a small compressive stress (peaking at 0.5 MPa) develops until 72 h. After 72 h, the specimen experiences monotonic shrinkage and a tensile stress of approximately 6.0 MPa has developed in the specimen at 14 days. The

mixture cured at 23 °C does not show substantial stress development until 14 h. After this time, the measured residual stress continues to increase as the specimen shrinks, until a residual stress around 3.7 MPa is measured at 7 days. It should be noted, a larger magnitude of residual stress develops at 10 °C than at 23 °C partially due to the higher strength developed at lower temperatures at an equivalent age (see Section 5.3) [1,11,12]. The mixture cured at 36 °C shows a rapid development in stresses from 4 to 5 h, after which the stress level plateaus. This corresponds to the interval of the expansion experienced by this mixture (Fig. 2a). A peak tensile stress of approximately 2.5 MPa develops in this mixture at 14 h, when the specimen fails with visible cracking.

Fig. 3b shows residual stress development in SRA mixtures cured at 10, 23 and 36 °C. In the mixture cured at 10 °C, a compressive stress develops around 20 h and is noted to persist until 114 h; with a peak compressive stress of 1.5 MPa being measured at 72 h. A peak tensile stress of 2.5 MPa is measured in this specimen at 14 days, which corresponds to the net shrinkage experienced by this specimen at 14 days (Fig. 2b). The specimen cured at 23 °C starts to develop compressive stresses at 9 h that peak at 1.0 MPa at an age of 18 h. After 28 h, a tensile stress begins to develop reaching 2.6 MPa at 7 days. In the mixture cured at 36 °C, tensile stresses begin to develop around 5 h and continuously increase until the specimen fails at 29 h at a peak tensile stress of 2.5 MPa. Globally, it is observed that the rate of residual stress development increases with an increase in the curing temperature. Further, all the mixtures experience early deformations which result in

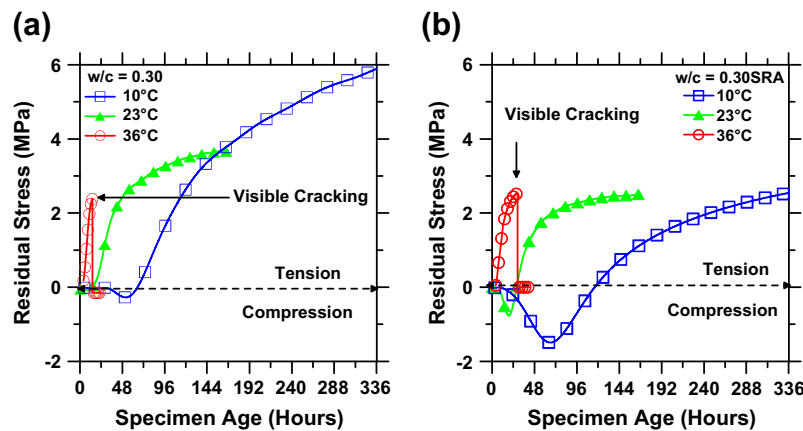


Fig. 3. The residual stress developed as a function of specimen age for cement pastes cured at different temperatures for: (a) plain pastes and (b) SRA containing pastes.

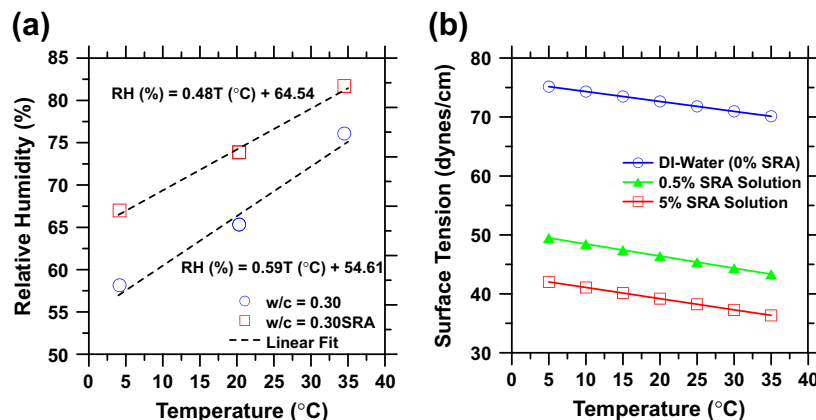


Fig. 4. The influence of temperature on: (a) Internal equilibrium relative humidity measured on mature, well-hydrated, sealed cement pastes and (b) Solution's surface tension for solutions containing three different concentrations of a shrinkage reducing admixture. The smaller slope (reduced RH–T sensitivity) of the SRA containing mixture as compared to the plain mixture (0.48%/°C vs. 0.59%/°C) seen in Fig. 4a suggests that these mixtures are less sensitive to thermal expansions than plain mixtures [50].

negligible stress development, conceivably due to stress relaxation and the low modulus of the material at these early ages. It should also be noted, over time, the residual stresses developed due to autogenous shrinkage are expected to be slightly higher in the plain mixtures than in the SRA mixtures, as the plain mixture will self-desiccate to a lower equilibrium relative humidity; see Fig. 4a [47–49].

#### 4.4. Autogenous RH of cement pastes and surface tension of solutions

Fig. 4a shows the internal equilibrium RH as a function of temperature measured on mature cement pastes using the Rotronic hygroscope. The internal RH is observed to decrease (or increase) linearly with decreasing (or increasing) temperature; however at a slightly higher rate for the plain mixture as compared to the SRA mixture. This is reasonable considering isotheric vapor pressure datasets compiled for pastes indicate that the RH–T relationship is relatively linear until intermediate humidities (until about RH = 50%) [50,51]. Further, the SRA mixture is observed to have a higher RH at a given temperature compared to the plain mixture due to the reduction in the surface tension of the pore solution by the SRA [49].

Fig. 4b shows the interfacial liquid–vapor surface tension measured using the du Noüy Ring method as a function of temperature for aqueous solutions containing several concentrations of a shrinkage reducing admixture (SRA). In general, it is noted that the surface tension decreases with increasing temperature. How-

ever, the rate of decrease in the surface tension is similar independent of SRA concentration. A similar trend in the surface tension behavior is observed in the case of synthetic (paste) pore solutions [40,49]. However, for the case at hand, the solution's surface tension is depressed with both an increase in the ionic-strength (i.e., concentration) and temperature [49]. The results provided in Fig. 6 are useful in quantifying the change in the capillary stress with temperature as described by the Young–Laplace Equation (Section 5.2).

## 5. Discussion of experimental results

### 5.1. The influence of temperature on the rate of cement hydration

The activation energy of cement hydration was determined using measurements of isothermal calorimetry at 10, 23 and 36 °C. The activation energy calculated using Eq. (1) assumes that mixtures cured at different temperatures take the same equivalent time to achieve an equivalent degree of hydration (cumulative energy release) [27]. Similar values obtained for the plain (36.2 kJ/mol) and SRA (37.8 kJ/mol) containing mixtures suggests that the addition of the SRA does not significantly influence the temperature sensitivity of cement hydration. Fig. 5 shows the energy release values measured using isothermal calorimetry that are maturity transformed using the apparent activation energy of cement hydration (reactions). Expectedly, upon applying the transformation, the

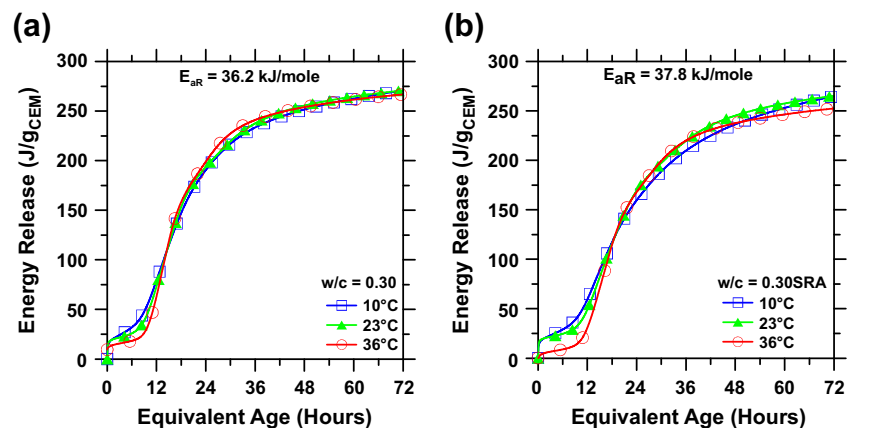


Fig. 5. The cumulative energy release as a function of equivalent specimen age for cement pastes cured at different temperatures for: (a) plain pastes and (b) SRA containing pastes.

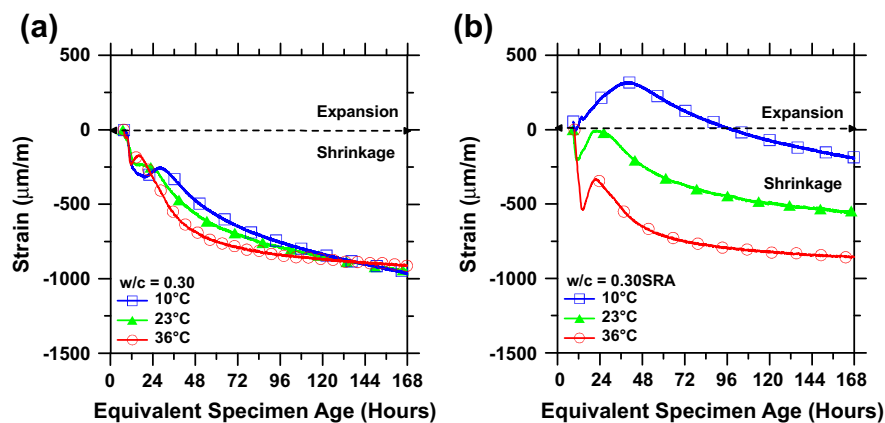


Fig. 6. Autogenous deformation from the time of set as a function of equivalent age for pastes cured at different temperatures for: (a) plain pastes and (b) SRA containing pastes. It should be noted that in spite of the seeming “visual-similarity” in the deformation profiles beyond 48 h, SRA containing mixtures cured at different temperatures show a consistently distinct shrinkage response from each other.



evolution and the final energy release value is similar for both the plain and SRA mixtures cured at different temperatures [52].

### 5.2. The influence of temperature on the driving forces of autogenous deformations: expansions, autogenous-RH change and the surface tension of the pore-fluids

Fig. 2 shows measurements of autogenous deformation zeroed to the time of final set. Here, it should be noted that the uncertainty related to identifying the “exact” time of final set and the high rate of shrinkage at this time produce an error of about 150  $\mu\text{m/m}$  in the zeroed shrinkage response [53]. Fig. 6 shows the evolution of autogenous deformation at 10, 23 and 36 °C which is maturity-transformed using the activation energy of hydration. The plain paste (Fig. 6a) shows a slight expansion or a plateau in shrinkage up to an equivalent age of 24 h. Expectedly, this expansion occurs earliest and has the shortest duration for the mixture cured at 36 °C. The opposite is true for the mixture cured at 10 °C. The occurrence of this expansion likely corresponds to the formation of expansion inducing phases during hydration [37,46,49,54,55]. The mixture cured at 23 °C experiences a plateau in shrinkage after setting which is followed by monotonic shrinkage thereafter.

Fig. 6b shows deformation curves as a function of equivalent age for SRA mixtures cured at 10, 23 and 36 °C. Here, unlike the plain paste, maturity transformations are observed to be fully unsuccessful in describing the temperature dependent response. Specifically, for these systems, a vastly different pattern of deformation (i.e., expansion or shrinkage) is observed at different temperatures [37,56]. This is related to a confluence of temperature-linked effects including the: (1) cement hydration rate, (2) liquid–vapor surface tension, (3) internal relative humidity, (4) expansions linked to the saturation index of solid phases in solution and (5) the microstructural arrangement (i.e., pore-structure) of the system [12,22,37,46,49,57–60,62]. For example: a recent study has revealed that portlandite is a driver of early-age expansions in SRA containing systems [37,46]. At different temperatures, as the saturation level (index) of portlandite linked to changes in the ion activities, solubilities and solubility products of phases varies, the magnitude of expansive deformations developed varies accordingly [46,55,57–61]. However, this response is difficult to quantify precisely as the temperature-linked influence of the SRA on the composition of the pore solution (and thus expansions) is not yet clear. Further, the magnitude of expansive stresses has been noted to be highest when crystals precipitate in pores in the mesopore range [62,63]. If the microstructural arrangement and the pore structure vary with the curing temperature, the pore-size dictated evolution of expansive stresses would be complicated to predict. As such, though the maturity method is capable of predicting the degree of reaction, it is unable to describe other deformation processes (i.e., phase crystallization induced expansions<sup>1</sup>) which are driven by changes in the constitution of the pore solution and have a non-linear dependence on the curing temperature and/or the microstructure of the material.<sup>2</sup>

<sup>1</sup> Given the increasing solubility of portlandite with decreasing temperature, and the influence of the SRA on the composition of the pore solution, at a first approximation, it is expected that the saturation index of portlandite (which causes expansions [21,37,46]) would increase with decreasing temperature. This would suggest that the magnitude of the expansion should also amplify with decreasing temperature as noted in Fig. 4b. However, further efforts are needed to fully substantiate this point.

<sup>2</sup> Given the non-linear temperature-to-pore solution composition relation and the impact of the SRA on the dissolution and solubility of solid phases, the application of the maturity approach is not feasible. Furthermore, the maturity approach assumes that the microstructure of materials cured at different temperatures is identical. Obviously, this is not accurate. Due to these points, the application of the maturity approach is substantially limited.

The overall autogenous deformation response can be explained by considering, after setting, as crystallization pressures try to produce an expansion, the paste self-desiccates, producing a shrinkage inducing stress (i.e., negative pressure) in the pore-fluid. As the desiccation stress overwhelms the expansive stress, the system shrinks [46]. As such, the net deformation ( $\varepsilon_{AD}$ ) of a sealed cement paste is a function of two competing mechanisms, crystallization stresses which cause expansions and self-desiccation stresses which cause shrinkage. This response can be mathematically generalized as shown in Eq. (2):

$$\varepsilon_{AD} = f(\sigma_C, \sigma_S) \quad (2)$$

where  $\sigma_C$  is the expansive crystallization stress that develops and  $\sigma_S$  is the tensile capillary (shrinkage inducing) stress that develops in the pore fluid. Here, it is important to note that the presence of a SRA depresses the surface tension of the pore-fluids which limits self-desiccation and in turn autogenous shrinkage in a sealed system [46,49]. As the reduction in the RH is delayed and reduced in SRA systems [46,49], the expansion of the paste occurring due to crystallization is more evident in SRA containing pastes than in plain cement pastes, since it is not masked by simultaneous shrinkage induced due to self-desiccation. Further, since expansion (solid phase precipitation) and shrinkage (self-desiccation) effects have different temperature sensitivities (i.e., activation energies linked to self-desiccation or phase crystallization), SRA pastes show an autogenous deformation response to which traditional maturity methods cannot be applied. These aspects are discussed in further detail below.

The capillary (i.e., shrinkage inducing) stress ( $\sigma_S$ , MPa) that develops in a liquid-filled pore space during desiccation can be described using the Young–Laplace and Kelvin Equations as a function of the interfacial surface tension of the pore-fluid and the Kelvin radius, or as a function of the internal equilibrium relative humidity (RH) in the pores as described in Eq. (3) below [14]:

$$\sigma_S = -\frac{2\gamma_{LV} \cos(\theta)}{r_K} = -\frac{\ln(RH/a_W)RT}{V_M} \quad (3)$$

where  $a_W$  is the water-activity of the pore-fluid (unitless; assumed to be 1<sup>3</sup> [46,49]),  $\gamma_{LV}$  is the interfacial (liquid–vapor) surface tension (N/m) of the pore-fluid,  $r_K$  (m) is the radius of curvature of the liquid–vapor meniscus (the Kelvin radius),  $\theta$  (assumed to be 0° (see Footnote 3) [63]) is the solid–liquid contact angle [64],  $V_M$  (m<sup>3</sup>/mol) is the molar volume of the pore-fluid (assumed to be water, 18.02 cm<sup>3</sup>/mol),  $R$  (J/K·mol) is the ideal gas constant,  $T$  (K) is the thermodynamic temperature, and  $RH$  is the equilibrium relative humidity in the pores. An analysis of Eq. (3) suggests that for sealed systems when the overall degree of fluid-saturation and Kelvin radius (i.e., the degree of hydration (See Footnote 5)) is similar for plain and SRA systems, the main factor that influences the capillary stress is the change in the liquid–vapor surface tension or the internal RH as a function of temperature [49,14]. Here, it is noted that between 10 and 36 °C, while the surface tension of water decreases by about 6%, the surface tension of a 5% SRA solution decreases by around 12% (independent of hydration). This change in the surface tension translates to a proportional decrease in the capillary stress developed in both these systems with an increasing curing temperature [49,14]. The reorganization of Eq. (3) then yields the Kelvin–Laplace equation which relates the Kelvin radius (and the capillary stress) to the RH<sup>4</sup> in the pores:

<sup>3</sup> This is not strictly accurate, but the assumption is made in this paper for the sake of simplicity. In reality, a change in the temperature would alter both the contact angle and the water activity as related to the pore solution composition.

<sup>4</sup> Strictly speaking, the RH term represents the partial pressure of water vapor contained in the pores. However, for the case at hand, the relative humidity and the partial pressure of water vapor are assumed equivalent.

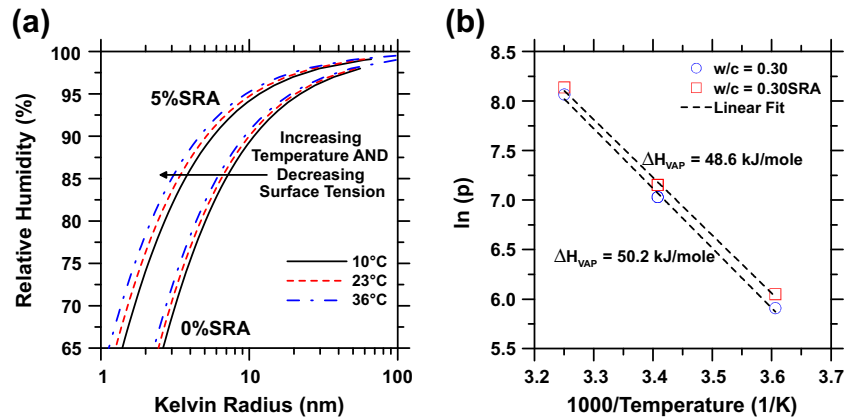


Fig. 7. A graphical interpretation of Eq. (4) which describes: (a) The relative humidity as a function of the critical Kelvin radius for different thermodynamic temperatures and (b) The enthalpy of vaporization ( $\Delta H_{VAP}$ ) for plain and SRA containing mixtures.

$$\ln\left(\frac{RH}{a_w}\right) = \left(\frac{-2\gamma_{LV}\cos(\theta)V_M}{r_K RT}\right) \quad (4)$$

From an analysis of Eq. (4), in a fashion analogous to Eq. (3), it can be concluded that when the Kelvin radius (e.g., 5 nm) is fixed as relevant for systems that hydrate to an equivalent extent (and have a similar liquid saturation level<sup>5</sup> [46,49,65,66]), as the curing temperature varies between 10 and 36 °C, the depletion RH varies between 79.8% and 82.3% for the plain system and 88.7% and 90.7% for the SRA containing system (Fig. 7a), suggesting that the capillary stress developed in fact increases with decreasing temperature as shown in Figs. 4a and 7a. However, in dynamic systems as applicable at early-ages, which hydrate and self-desiccate simultaneously, the expected (slight) increase in the capillary stress produced by lower (curing) temperatures is offset by the reduction in the rate of cement hydration and self-desiccation. This explains why though pastes cured at higher temperatures should shrink less, and systems cured at lower temperatures should shrink more (in line with the expected capillary stress response), a reduced rate of hydration at lower temperatures depresses the rate of autogenous RH decrease (resulting in a higher internal RH on a time-scale) ensuring that the capillary stress and the magnitude of shrinkage developed on a time-scale is also proportionally reduced at lower temperatures.<sup>6</sup> This response is also additionally impacted by: (1) the slightly higher strength of systems cured at lower temperatures [1,58,67] (which provides more resistance to shrinkage) and the lower rate of capillary stress application as linked to the cement reaction rate as discussed further in Section 5.3<sup>7</sup> and (2) the coarsening of the cement paste's microstructure at elevated temperatures which would act to reduce the magnitude of autogenous stresses developed in the system [12].

Fig. 4a shows the change in the equilibrium RH with temperature for mature, plain and SRA pastes. This RH–T dependence

(Fig. 7b) can be interpreted using the Clausius–Clapeyron relation to quantify the enthalpy (i.e., heat) of vaporization, the driving force for the liquid–vapor phase transition of the physically-bound (i.e., evaporable) water in the material:

$$RH(\%) = p/p_s \times 100 \quad (5a)$$

$$\ln(p) = \frac{-\Delta H_{VAP}}{RT} + C \quad (5b)$$

where  $p$  is the partial vapor pressure of water vapor (mm-Hg),  $p_s$  is the saturated vapor pressure of water vapor (mm-Hg) at a given temperature [68],  $\Delta H_{VAP}$  is the enthalpy (heat) of vaporization of the evaporable-water (kJ/mol),  $R$  is the ideal gas constant (8.314 J/K-mol),  $T$  is the thermodynamic temperature (K) and  $C$  is an integration constant (unitless). It should be noted that this calculation considers water vapor as an ideal gas and neglects the presence of ions in the pore-fluid. The slope of a linear function fit to the experimental vapor pressure data (Fig. 4a) yields the enthalpy of vaporization; 50.2 and 48.6 kJ/mol for the plain and SRA mixtures, respectively. These values are slightly higher than the value reported for liquid water at 23 °C, 44 kJ/mol [68], due to the presence of ions or a change in the difference in the thermodynamic properties of water contained in the cement paste [69,70]. The SRA system has a slightly lower enthalpy likely due to the presence of the SRA which reduces the surface tension of the solution and facilitates evaporation [71]. This relationship up on being quantified permits estimation of the equilibrium RH in the pores over a specific range of temperature change. Further, it describes the temperature dependence of self-desiccation (i.e., autogenous-RH change), which invalidates the application of the traditional maturity method to autogenous effects due to its dependence on both the rate of cement hydration and the curing temperature. In spite of the additional effort, the enthalpy of vaporization information only partially enables application of a multi-part [27,72] activation energy (i.e., equivalent age) type correction based on the cement reaction rate and the temperature dependence of self-desiccation as considerations linked to porestructural changes and expansions as relevant to autogenous deformations are yet not considered in the approach.

In closing, the elastic deformation (i.e., expansion or shrinkage) experienced by a cementitious material can be described as a function of the degree of phase-saturation, the stress developed (shrinkage or expansive stress) and the elastic properties as described using Eq. (6) [73]:

$$\varepsilon_{AD} = \frac{(S_C \sigma_C - S_L \sigma_S)}{3} \left( \frac{1}{K_B} - \frac{1}{K_S} \right) \quad (6)$$

<sup>5</sup> Isothermal calorimetry measurements broadly indicate that the extent of hydration of the plain and SRA systems is similar after 24 h; i.e., within ±5%. Since water consumption is driven by cement hydration, a similar extent of hydration implies a similar liquid saturation level in the system. If the plain and SRA pastes have a similar pore system [65,66], it would be expected that the available liquid water is contained in pores of a similar nature (size range); implying an “equivalent” (fixed) saturated Kelvin (pore) radius. As such, the sizes of pores that are expected to be water-filled or empty (i.e., liquid saturation) is assumed equivalent for these systems at a similar extent of reaction.

<sup>6</sup> It should be noted however, that this analysis disregards (ion/water) activity effects which influence both, the internal RH and the surface tension of the solution. Further research is needed to examine these effects in more detail.

<sup>7</sup> This is only true for systems which do not show expansion phenomena which are influenced by temperature differently from shrinkage. If the expansion has its own temperature sensitivity, this complicates the prediction of the shrinkage response.

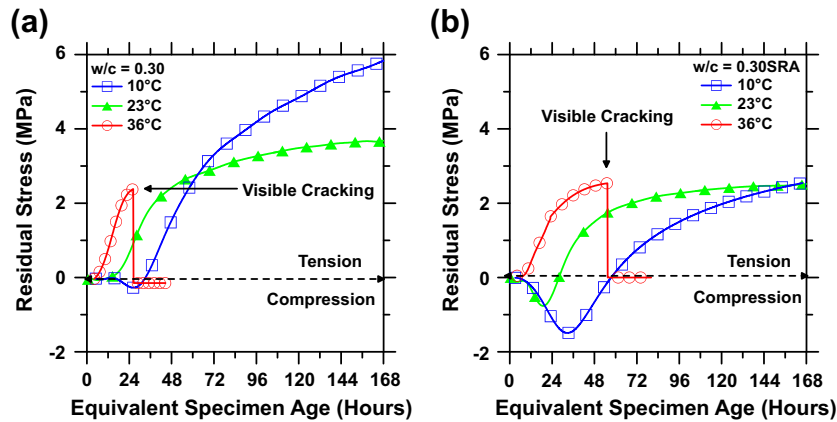


Fig. 8. Residual stress developed as a function of equivalent age for cement pastes cured at different temperatures for: (a) plain pastes and (b) SRA containing pastes.

where  $\varepsilon_{AD}$  is the net linear deformation experienced by the paste ( $\mu\text{m}/\text{m}$ ),  $S_L$  is the degree of liquid-saturation (i.e., fraction of the pore space occupied by the pore-fluid, unitless),  $S_C$  is the fraction of the pore space occupied by expansion causing crystals (unitless),  $\sigma_C$  (MPa) is the expansive stress developed due to phase crystallization and  $\sigma_S$  (MPa) is the shrinkage inducing stress produced due to self-desiccation,  $K_B$  is the bulk modulus of the body including the effects of the porosity (GPa) and  $K_S$  is the bulk modulus of the solid skeleton (assumed constant as 44 GPa) [74,75]. While the temperature dependence of the capillary and crystallization stresses has been described, the temperature sensitivity of the other terms requires clarification. First, the molar volume ( $V_M$ ) of water increases with temperature. The Kelvin equation indicates a higher RH (Fig. 7a) at higher temperatures suggesting that smaller pores may yet remain filled with increasing temperature, indicating a higher liquid saturation level. However, given the small change in the liquid-saturation term (ranging between 0.8 and 1.0 for sealed systems at early-ages), this is a 2nd order effect that can be neglected initially. Second, while the bulk (elastic) modulus is macroscopically maturity-transformable (Eq. (1) and Fig. 9a), any changes induced in the porosity and the arrangement of the reaction products may complicate this response [5,76,77]. Similar considerations will impact the skeletal modulus ( $K_S$ ) as related to compositional changes in the C–S–H and the arrangement and/or mass balance of the cement hydrates with temperature [57,58,78–80]. In summary, this discussion comprehensively describes why traditional maturity (equivalent age) approaches are an inappropriate method to describe the influence of temperature on autogenous deformations in cementitious materials.

### 5.3. The influence of temperature, viscoelasticity and damage on stress development

Fig. 8 shows maturity transformed residual stress profiles for paste mixtures undergoing sealed hydration. Here, it is noted that traditional maturity transformations are unsuccessful at all temperatures (for both mixtures) and the rate of residual stress development increases with increasing temperature. This observation can be explained by a combination of several effects including the evolution of autogenous deformations, viscoelastic effects (i.e. age of loading and the rate of loading) and damage development (microcracking) at different temperatures. This can be explained by considering that the stress ( $\sigma_R$ , MPa) developed up on the restrained deformation of a cement paste (as applicable for the ring tests) is a function of: (1) the magnitude of the imposed deformation (expansion/shrinkage) and the extent of stress relaxed and relieved due to (2) viscoelastic effects and (3) microcracking. This relation is generalized in Eq. (7):

$$\sigma_R = f(\sigma_{AD}, \sigma_{VE}, \sigma_{MC}) \quad (7)$$

where  $\sigma_{AD}$  is the elastic stress developed due to the restraint of (free) autogenous volume change (shrinkage/expansion, MPa),  $\sigma_{VE}$  is the magnitude of stress relaxed due to viscoelastic (creep) deformations (MPa) and  $\sigma_{MC}$  is the magnitude of stress relaxed due to microcracking (MPa).

Since cement paste is an aging nonlinear viscoelastic material, this results in substantial stress relaxation in restrained pastes at early ages. When a shrinkage load is imposed on the paste, the amount of stress that is relaxed is based on the duration of loading

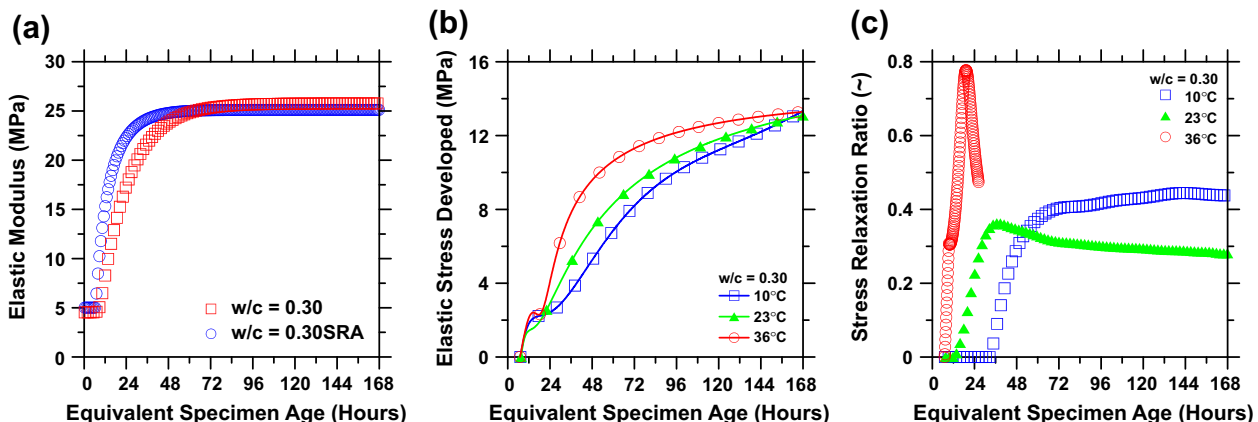


Fig. 9. The evolution of the: (a) elastic modulus [86], (b) restrained elastic stress and (c) stress relaxation coefficient as a function of equivalent age for the plain paste ( $w/c = 0.30$ ).



and on the maturity of the specimen (stiffness) at the time (age) the load is applied. In the case of stress developed due to restrained deformation, the rate of stress development also matters, which depends on the rate of deformation of the paste and its elastic stiffness. First, simple maturity transformations cannot be used to transform the residual stress developed, as while a maturity transformation incorporates the variable specimen age (i.e., maturity as related to stiffness or strength; Fig. 9a) at loading, such methods are incapable of transforming the duration over which the load is applied (i.e., the rate of capillary stress loading which drives the rate of shrinkage and stress development). As such, materials cured at higher temperatures are under load for a shorter duration and experience less stress relaxation while specimens at a lower temperature can exhibit substantially more stress relaxation (Fig. 9c).

The argument of reduced stress relaxation at higher temperatures is clearly substantiated by an examination of Fig. 9c which describes the stress relaxation ratio, i.e., the ratio of the measured residual to the calculated elastic stresses<sup>8</sup> [81–83]. It is noted that cement pastes cured at higher temperatures, which hydrate and shrink faster (i.e., are loaded faster) are unable to substantially relax shrinkage stresses (viscoelastically, due to the higher rate of load application) which may suggest that these pastes likely develop more distributed damage (microcracks) as a mechanism of stress relaxation.<sup>9</sup> A similar rate/extent of shrinkage dependent response has also been noted in pastes made of cements of differing finenesses which hydrate at different rates in a fashion analogous to a temperature dependent effect [84]. This potentially explains why materials cured at higher temperatures develop and fail at lower residual stresses, as given the larger extent of damage/microcracking (and the lower strength) of these systems, microcracks are able to progressively accumulate with increasing shrinkage and release stresses, but also coalesce more readily to form macroscopic cracks, when the specimen fails (Fig. 8) [83,85]. However, at lower temperatures, since the cement paste is loaded later and more slowly, shrinkage stresses can be more readily relaxed through creep effects. As such, less stress is dissipated in the form of distributed damage, resulting in less microcracking (damage) in the material. This is an important point as a smaller extent of microcracking ensures that materials cured at lower temperatures are in effect more (damage) resistant to macroscopic (i.e., unstable crack extension) damage localization (Figs. 3 and 8). These aspects of viscoelastic and damage (microcracking) effects which are not considered in the traditional maturity approach invalidate its use to describe the influence of temperature on stress development in cementitious materials.

## 6. Summary and conclusions

This research has comprehensively studied the influence of temperature on the rate of cement hydration, autogenous deformations and residual stress development under sealed conditions. The apparent activation energy of cement hydration has been quantified using isothermal calorimetry. The activation energy

thus determined was found to be 36.2 kJ/mol and 37.8 kJ/mol for the plain and SRA containing mixtures respectively. The similarity in the activation energy suggests that the addition of a SRA does not appreciably influence the temperature sensitivity of cement hydration.

It has been demonstrated that, while on certain occasions maturity transformations may be able to describe the influence of temperature on autogenous deformations for certain (plain) cement pastes, within a restricted temperature range, in general they are an inappropriate approach to represent the influence of temperature on autogenous deformations in (expansive) cementitious materials containing SRAs. From a conceptual basis, this is principally because the application of the maturity approach is erroneous to predict any material property which shows a dependence on a parameter other than the cement reaction (hydration) rate. In the case of autogenous deformations, the varying temperature sensitivity related to the cement reaction rate, autogenous RH change, interfacial surface tension, expansive processes and pore-structural effects cannot be captured by the singular application of a maturity transformation. Further, it is shown that stress development, in sealed systems, cured at different temperatures can also not be described using a maturity function for any set of mixtures (cement chemistries) or environmental conditions. This point is related to the inability to suitably maturity transform autogenous deformations and incremental complications related to damage (microcracking) and viscoelastic considerations which depend on the age at which and the duration over which a load (i.e., capillary stress) is applied on a sealed desiccating system.

## Acknowledgements

The author is profoundly grateful to Professor Jason Weiss (Purdue University) and Professor Pietro Lura (EMPA/ETHZ) for several years of constructive advice, valuable discussions and tremendous mentoring. The author gratefully acknowledges financial support for this research received during a M.S./Ph.D. studentship at Purdue University from the Purdue Research Foundation, BASF Construction Chemicals and the National Science Foundation's Science and Technology Center for Advanced Cement-Based Materials at Purdue University. This work was conducted in the Materials Characterization and Sensing Laboratory at Purdue University and the Laboratory for Concrete and Construction Chemistry at the Swiss Federal Laboratories for Materials Science and Technology and as such the author would like to acknowledge the support that has made these laboratories and their operation possible. The author would like to thank Dale Bentz (NIST) for useful advice, insightful comments and a comprehensive review of this paper, Professor Karen Scrivener (EPFL) for scientific discussions and Daniel Matson (Purdue University) for his extensive and dedicated efforts in carrying out the experimental evaluations. The contents of this paper reflect the views of the author, who is responsible for the accuracy of the datasets presented herein.

## References

- [1] Carino NJ. The maturity method. In: Malhotra VM, Carino NJ, editors. CRC handbook on nondestructive testing of concrete. Boca Raton, Florida: CRC Press; 1991. p. 101–146.
- [2] Weiss WJ. The Experimental determination of the 'Time Zero'. In: Bentur editor. RILEM STAR TC-EAS: early age cracking in cementitious systems A; 2003. p. 195–206.
- [3] Pinto RCA, Hover KC. Application of the maturity approach to setting time. *ACI Mater J* 1999;96(6):686–91.
- [4] Roy DM, Scheetz BE, Sabol S, Brown PW, Shi D, Licastro PH, Idorn GM, Andersen PJ, Johanson V. The maturity model and curing technology. Strategic highway research, Program. SHRP-C-625.
- [5] Barde A, Mazzotta G, Weiss WJ. Early-age flexural strength: the role of aggregates and their influence on maturity predictions. In: Material science of concrete VII. American Ceramic Society, Wiley Publishers; 2005. p. 12.

<sup>8</sup> The total elastic stress is computed using the incremental unrestrained volume change of the paste, the elastic properties of the invar and cement paste and the geometrical description of the ring setup. For detailed descriptions, the reader is referred to the work of Hossain and Weiss [81].

<sup>9</sup> First, while it may be argued that creep reduces with temperature, given the limited variation in creep for the temperature range of interest, a larger extent of stress relaxation is enabled at lower temperatures due to the increasing compliance and the lower rate of deformation of the material. Second, this argument does not consider the impact of temperature on the strength of the material. More detailed analysis may indicate that while the initial flaw size in these materials is similar and independent of the curing temperature (being similar in magnitude to the size of the largest cement particle [6]), the critical flaw size which dictates failure varies, increasing with decreasing temperature given the increased strength of cementitious materials cured at lower temperatures.

- [6] Mindess S, Young JF, Darwin D. Concrete. 2nd Edn. New Jersey: Prentice Hall; 2003 [p. 656].
- [7] Nurse RW. Steam curing of concrete. *Mag Concr Res* 1949;1(2):79–88.
- [8] Saul AGA. Principles underlying the steam curing of concrete at atmospheric pressure. *Mag Concr Res* 1951;2(6):127–40.
- [9] Hansen PF, Pedersen EJ. Maturity computer for controlled curing and hardening of concrete. *Nordisk Betong* (In Danish) 1977;1:21–5.
- [10] Arrhenius S. On the reaction velocity of the inversion of cane sugar by acids. *Z Phys Chem* 1889;4:226.
- [11] Bentur A. Effect of curing temperature on the pore structure of tricalcium silicate pastes. *J Colloid Interface Sci* 1979;74(2):549–60.
- [12] Thomas JJ, Jennings HM. Effect of heat treatment on the pore structure and drying shrinkage behavior of hydrated cement paste. *J Am Ceram Soc* 2002;85(9):2293–8.
- [13] Lura P, Jensen OM. Measuring techniques for autogenous strain of cement paste. Portland cement association, PCA R&D Serial No. 2925, Skokie, IL; 2005, p. 26.
- [14] Lura P, Jensen OM, van Breugel K. Autogenous shrinkage in high-performance cement paste: an evaluation of basic mechanisms. *Cem Concr Res* 2003;33(2):223–32.
- [15] Shoya M, Sugita S, Sugiura T. Improvement of drying shrinkage and shrinkage cracking of concrete by special surfactant. In: Vázquez E, editor. *Admixtures for concrete: improvement of properties*. London; Chapman and Hall; 1990. p. 484–95.
- [16] Balogh A. New admixture combats concrete shrinkage. *Concr Cons* 1996(July).
- [17] Nmai C, Tomita R, Hondo F, Buffenbarger J. Shrinkage reducing admixtures. *Concr Int* 1998;20(4):31–7.
- [18] Berke NS, Dallaire MC, Hicks MC, Kerker A. New developments in shrinkage-reducing admixtures, superplasticizers and other chemical admixtures in concrete. In: *Proceedings fifth CANMET/ACI international conference*, Rome, Italy; 1997, p. 971–988.
- [19] Shah SP, Weiss WJ, Yang W. Shrinkage cracking – can it be prevented? *Concr Int* 1998;20(4):51–5.
- [20] Bentz DP. Curing with shrinkage-reducing admixtures: beyond drying shrinkage reduction. *Concr Int* 2005;27(10):51–60.
- [21] Rajabipour F, Sant G, Weiss WJ. Interactions between shrinkage reducing admixtures and cement paste's pore solution. *Cem Concr Res* 2008;38(5):606–15.
- [22] Jensen OM, Hansen PF. Influence of temperature on autogenous deformation and relative humidity change in hardening cement paste. *Cem Concr Res* 1999;29(4):567–75.
- [23] Lura P. Autogenous deformation and internal curing of concrete. PhD thesis, Delft University of Technology, Delft, the Netherlands; 2003.
- [24] Lura P, van Breugel K, Maruyama I. Effect of curing temperature and type of cement on early-age shrinkage of high-performance concrete. *Cem Concr Res* 2001;31(12):1867–72.
- [25] Tuncry P, Loukili A, Barcelo L, Casabonne JM. Can the maturity concept be used to separate the autogenous shrinkage and thermal deformation of a cement paste at early age? *Cem Concr Res* 2002;32(9):1443–50.
- [26] Bjøntegaard Ø. Thermal dilation and autogenous deformation as driving forces to self-induced stresses in high-performance concrete. PhD thesis, NTNU, Division of Structural Engineering, Norway; 1999.
- [27] Sant G, Weiss WJ. Applications that require a correction before the maturity concept is applied. In: *International RILEM conference on microstructure related durability of cement based composites 'Microdurability2008'*, China; 2008, p. 765–774.
- [28] Sant G, Lura P, Weiss WJ. The influence of temperature on unrestrained volume changes in cementitious materials. In: *International RILEM conference on concrete durability and service life planning 'ConcreteLife '09'*, Haifa, Israel; 2009.
- [29] Sant G, Lura P, Weiss WJ. Measurement of volume change in cementitious materials at early ages: review of testing protocols and interpretation of results. *Transport Res Rec* 2006;1979:21–9.
- [30] Sant G, Ferraris CF, Weiss WJ. Rheological properties of cement pastes: a discussion of structure formation and mechanical property development. *Cem Concr Res* 2008;38(11):1286–96.
- [31] Jensen OM, Hansen PF. Water-entrained cement-based materials: I, principles and theoretical background. *Cem Concr Res* 2001;31(5):647–54.
- [32] Bentz DP. A three-dimensional cement hydration and microstructure program I – hydration rate, heat of hydration, and chemical shrinkage, NISTIR 5756, US Department of Commerce, USA; 1995.
- [33] Jensen OM, Hansen PF. A dilatometer for measuring autogenous deformation in hardening portland cement paste. *Mater Struct* 1995;28(181):406–9.
- [34] Sant G, Lura P, Weiss WJ. A discussion of analysis approaches for determining 'time-zero' from chemical shrinkage and autogenous strain measurements in cement pastes. In: Jensen OM, Lura P, Kovler K. editors. *RILEM international conference 'volume changes of hardening concrete'*, Denmark; 2006, p. 375–384.
- [35] Sant G. Examining volume change, stress development and cracking in cement-based materials' Master's Thesis, Purdue University, West Lafayette, IN, USA; 2007, p. 235.
- [36] Sant G, Rajabipour F, Lura P, Weiss J. Examining residual stress development in cementitious materials experiencing an early-age expansion. In: *9th CANMET-ACI international conference – T.C. Holland Symposium*, Warsaw, Poland; 2007.
- [37] Sant G. Fundamental investigations related to the mitigation of volume changes in cement-based materials at early ages. PhD Dissertation, Purdue University, West Lafayette, IN, USA; 2009, p. 226.
- [38] Jensen OM, Hansen PF. Autogenous relative humidity change in silica fume-modified cement paste. *Adv Cem Res* 1995;7(25):33–8.
- [39] Adamson AW. Physical chemistry of surfaces, Wiley, New York; 1990, p. 777.
- [40] Sant G, Eberhardt A, Bentz DP, Weiss WJ. The influence of shrinkage reducing admixtures (SRAs) on moisture movement in cementitious materials at early ages. *The ASCE J Mater Civil Eng* March 2010;22(3):10.
- [41] Weast RC, Astle MJ, Beyer WH. CRC handbook of chemistry and physics. 88th Edn. CRC Press; 2007 [p. 2640].
- [42] Pease BJ. The role of shrinkage reducing admixtures on shrinkage, stress development, and cracking. MSCE Thesis, Purdue University, West Lafayette, Indiana, USA; 2005, p. 236.
- [43] Rajabipour F. 'Insitu Electrical Sensing and Material Health Monitoring in Concrete Structures', pp. 193, PhD Dissertation, Purdue University, West Lafayette, IN, USA, (2006).
- [44] Sant G, Rajabipour F, Lura P, Weiss J. Examining time-zero and early age expansions in pastes containing shrinkage reducing admixtures. In: *2nd RILEM symposium on advances in concrete through science and engineering*; 2006, p. 11.
- [45] Scherer GW. Stress from crystallization of salts. *Cem Concr Res* 2004;34(9):1613–24.
- [46] Sant G, Lothenbach B, Juilland P, LeSaout G, Weiss WJ, Scrivener K. The origin of early-age expansions in pastes containing shrinkage reducing admixtures. *Cem Concr Res* 2011;41(3):218–29.
- [47] Bentz D, Geiker M, Hansen K. Shrinkage reducing admixtures and early-age desiccation in cement pastes and mortars. *Cem Concr Res* 2001;31(7):1075–85.
- [48] Sant G, Rajabipour F, Lura P, Weiss WJ. Volume changes in pastes containing shrinkage reducing admixtures under autogenous and drying conditions. In: *12th international congress on the chemistry of cement (electronic proceedings)*, Montreal, Canada; July 2007.
- [49] Weiss WJ, Lura P, Rajabipour F, Sant G. Performance of shrinkage reducing admixtures at different humidities and at early ages. *ACI Mater J* 2008;105(5):478–86.
- [50] Loser R, Di Bella C, Münch B, Lura P. Measuring the coefficient of thermal expansion of cement paste at early age. *Service Life Design for Infrastructure*, Delft, the Netherlands, RILEM PRO 2010; 70(2): p. 707–714.
- [51] Radjy F, Sellevold EJ, Hansen KK. Isothermic vapor pressure–temperature data for water sorption in hardened cement paste: enthalpy, entropy and sorption isotherms at different temperatures. Report: BYG-DTU-057, Technical University of Denmark, Lyngby, Denmark; 2003, p. 58.
- [52] Boivin S, Acker P, Rigaud S, Clavaud B. Experimental assessment of chemical shrinkage of hydrating cement pastes. In: Tazawa E. editor. *International workshop on autogenous shrinkage of concrete 'Autoshrink 98'*, Japan; 1998.
- [53] Sant G, Dehadrai M, Bentz D, Lura P, Ferraris CF, Bullard JW, et al. Detecting the fluid-to-solid transition in cement pastes: comparing experimental and numerical techniques. *Concr Int* 2009;31(6):53–8.
- [54] Skibsted J, Jensen OM, Jakobsen HJ. Hydration kinetics for the alite, belite, and calcium aluminate phases in portland cements from 27Al and 29Si MAS-NMR spectroscopy. In: *10th international congress on the chemistry of cements*, Göteborg; 1997.
- [55] Taylor HFW. Cement chemistry. 2nd Edn. London: Thomas Telford; 1997.
- [56] Cohen MD. Theories of expansion in sulfoaluminate-type expansive cements: schools of thought. *Cem Concr Res* 1983;13:809–18.
- [57] Lothenbach B, Matschei T, Moschner G, Glasser FP. Thermodynamic modeling of the effect of temperature on the hydration and porosity of Portland cement. *Cem Concr Res* 2008;38(1):1–18.
- [58] Lothenbach B, Winnefeld F, Alder C, Wieland E, Lunk P. Effect of temperature on the pore solution, microstructure and hydration products of Portland cement pastes. *Cem Concr Res* 2007;37(4):483–91.
- [59] Flatt RJ, Scherer GW. Thermodynamics of crystallization stresses in DEF. *Cem Concr Res* 2008;38:325–36.
- [60] Mounanga P, Baroghel-Bouny V, Loukili A, Khelidj A. Autogenous deformations of cement pastes: Part 1. Temperature effects at early age and micro-macro correlations. *Cem Concr Res* 2006;36(1):110–22.
- [61] Baroghel-Bouny V, Mounanga P, Khelidj A, Loukili A, Rafai N. Autogenous deformations of cement pastes: Part 2. W/C effects, micro-macro correlations and threshold values. *Cem Concr Res* 2006;36(1):123–36.
- [62] Scherer G. Crystallization in pores. *Cem Concr Res* 1999;29(8):1347–58.
- [63] IUPAC. Manual of symbols and terminology: Appendix 2, Part 1: colloid and surface chemistry. *J Pure Appl Chem* 1972; 31: 578.
- [64] Bentz DP. Influence of shrinkage-reducing admixtures on early-age properties of cement pastes. *J Adv Concr Technol* 2006;4(3):423–9.
- [65] Sant G, Bentz DP, Weiss WJ. Capillary depercolation in cement-based materials: measurement techniques and factors which influence their interpretation. *Cem Concr Res*, in press, p. 11, doi:10.1016/j.cemconres.2011.04.006.
- [66] Sant G, Lovell J, Weiss WJ. Mercury intrusion porosimetry of ordinary portland cement pastes: unpublished results, Purdue University, West Lafayette, IN; 2006–2009.
- [67] Price WH. Factors influencing concrete strength. *J Am Concr Inst* 1951;47(31):417–32.
- [68] The thermodynamic properties of water. [http://en.wikipedia.org/wiki/Water\\_\(data\\_page\)](http://en.wikipedia.org/wiki/Water_(data_page)). last verified July 22; 2009.

- [69] Apelblat A, Korin E. The vapor pressures of saturated aqueous solutions of sodium chloride, sodium bromide, sodium nitrate, sodium nitrite, potassium iodate, and rubidium chloride at temperatures from 227 K to 323 K. *J Chem Thermodyn* 1998;30:59–71.
- [70] Apelblat A, Korin E. Vapor pressures of saturated aqueous solutions of ammonium iodide, potassium iodide, potassium nitrate, strontium chloride, lithium sulfate, sodium thiosulfate, magnesium nitrate, and uranyl nitrate from  $T = (278–323)$  K. *J Chem Thermodyn* 1998;30:459–71.
- [71] Lura P, Pease B, Mazzotta G, Rajabipour F, Weiss WJ. Influence of shrinkage-reducing admixtures on development of plastic shrinkage cracks. *ACI Mater J* 2007;104(2):187–94.
- [72] Sant G, Rajabipour F, Weiss WJ. The influence of temperature on electrical conductivity measurements and maturity predictions in cementitious materials during hydration. *The Indian Concr J* 2008;23(April):1–8.
- [73] Bentz D, Garboczi EJ, Quenard DA. Modeling drying shrinkage in reconstructed porous materials: application to porous vycor glass. *Model Simul Mater Sci Eng* 1998;6:211–36.
- [74] Nielsen LF. A research note on sorption, pore size distribution and shrinkage of porous materials. Building Materials Laboratory, The Technical University of Denmark, Lyngby, Denmark, Technical, Report 245/91; 1991.
- [75] Grasley ZC, Scherer GW, Lange DA, Valenza JJ. Dynamic pressurization method for measuring permeability and modulus: II. cementitious materials. *Mater Struct* 2007;40:711–21.
- [76] Waller V, D'Aloia L, Cussigh F, Lecrux S. Using the maturity method in cracking control at early ages. *Cem Concr Compos* 2004;26(5):589–99.
- [77] Pane I, Hansen W. Concrete hydration and mechanical properties under nonisothermal conditions. *ACI Mater J* 2002;99(5):534–42.
- [78] Famy C, Scrivener KL, Crumbie AK. What causes differences of C–S–H gel grey levels in backscattered electron images? *Cem Concr Res* 2002;32(9):1465–71.
- [79] Kjellsen KO, Jennings HM. Observations of microcracking in cement paste upon drying and rewetting by environmental scanning electron microscopy. *Adv Cem Based Mater* 1996;3:14–9.
- [80] Escalante-Garcia JL, Sharp JH. Variation in the composition of C–S–H gel in Portland cement pastes cured at various temperatures. *J Am Ceram Soc* 1999;82(11):3237–41.
- [81] Hossain A, Weiss WJ. Assessing residual stress development and stress relaxation in restrained concrete ring specimens. *Cem Concr Comp* 2004;26(5):531–40.
- [82] Hossain A, Weiss WJ. Effect of specimen geometry and boundary conditions on stress development and cracking in the restrained ring test. *Cem Concr Res* 2006;36(1):189–99.
- [83] Hossain AB, Pease B, Weiss WJ. Quantifying restrained shrinkage cracking potential in concrete using the restrained ring test with acoustic emission. *Transport Res Rec, Mater Constr* 2003;1834:24–33.
- [84] Bentz D, Sant G, Weiss WJ. Early-age properties of cement-based materials: I. Influence of cement fineness. *The ASCE J Mater Civil Eng* 2008;20(7):502–8.
- [85] Kim B, Weiss WJ. Using acoustic emission to quantify damage in restrained fiber-reinforced cement mortars 2003; 33(2): p. 207–214.
- [86] Dehadrai M. Health monitoring of civil engineering materials. MSCE Thesis, Purdue University, West Lafayette, IN, USA; 2008, p. 201.